

Viral Serine Palmitoyltransferase Induces Metabolic Switch in Sphingolipid Biosynthesis and is required for Infection of a Marine Alga

Carmit Ziv, Sergey Malitsky, Alaa Othman, Shifra Ben-Dor, Yu Wei, Shuning Zheng, Asaph Aharoni, Thorsten Hornemann, and Assaf Vardi

Supporting Information Appendix

Supporting Tables

Table S1: LCB content as % of total LCB analyzed for each sample

Table S2: Primers used in this study

Supporting Figures

Figure S1: Mass-spec identification of vSPT protein resolved on SDS-PAGE

Figure S2: Viral SPT is highly expressed at early stages of viral infection

Figure S3: Viral infection induces a shift in substrate specificity of SPT *in vitro*

Figure S4: *de novo* LCB synthesis by the virus is required for viral assembly

Figure S5: LCB profile during viral infection

Figure S6: Putative structural elucidation of t17:0 after acid and base hydrolysis and derivatization with o-phathaldelyde

Figure S7: Viral infection induces the formation of C17 linear LCB and not C17 iso-branched

Figure S8: LC-MS putative identification of t17-vGSL (Glu-t17:0;h22:0)

Figure S9: LC-MS analysis of t17-vGSL (Glu-t17:0;h22:0) with ESI+

Figure S10: LC-MS analysis of t17-vGSL (Glu-t17:0;h22:0) with ESI-

Figure S11: 3-Keto-Dihydrosphingosines (KDS) with 16 or 17 carbons in length were accumulated during viral infection

Supporting Methods

References

Supporting Tables

Supporting Table S1: LCB content as % of total LCB analyzed for each sample (numbers indicate hpi). Elemental composition and mass of the protonated compound [M+H] are presented.

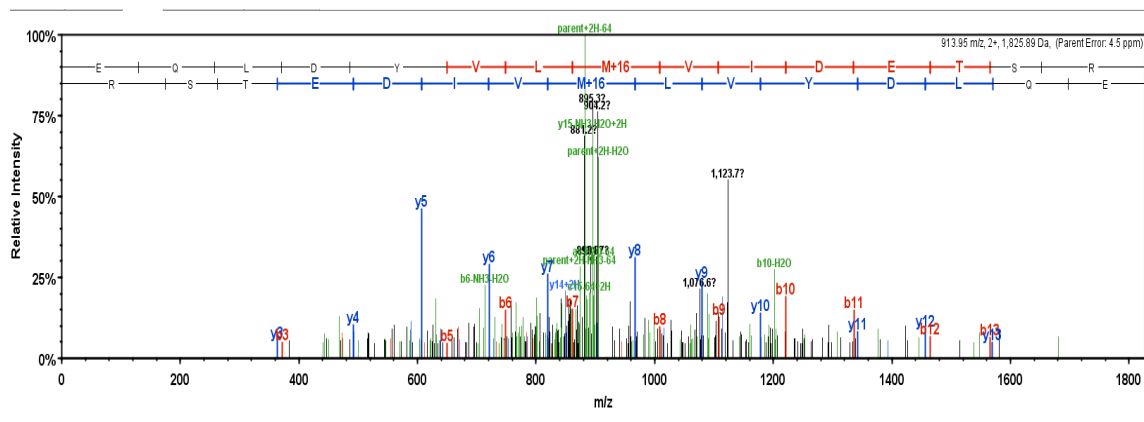
Analyte	Elemental composition	[M+H] (m/z)	Control	Control + myriocin	Infected cells				Infected cells + myriocin			
			24	24	6	12	24	48	6	12	24	48
t16:0	C ₁₆ H ₃₅ NO ₃	290.270	0.0%	0.0%	0.1%	0.3%	2.7%	7.0%	0.0%	0.0%	0.0%	0.0%
d16:0	C ₁₆ H ₃₅ NO ₂	274.275	0.1%	0.1%	0.2%	0.4%	0.5%	0.7%	0.1%	0.1%	0.1%	0.1%
d16:1	C ₁₆ H ₃₃ NO ₂	272.259	0.7%	0.7%	0.6%	0.7%	0.5%	0.4%	0.7%	0.8%	0.7%	0.7%
t17:0	C ₁₇ H ₃₇ NO ₃	304.285	0.0%	0.0%	0.4%	2.0%	18.7%	31.2%	0.0%	0.1%	0.1%	0.2%
d17:0	C ₁₇ H ₃₇ NO ₂	288.290	0.1%	0.1%	0.2%	0.3%	0.8%	1.4%	0.1%	0.1%	0.1%	0.1%
d17:1	C ₁₇ H ₃₅ NO ₂	286.275	3.7%	3.5%	3.8%	3.6%	2.6%	2.0%	3.8%	3.8%	3.8%	3.9%
t18:0	C ₁₈ H ₃₉ NO ₃	318.301	0.0%	0.0%	0.2%	0.6%	3.3%	5.6%	0.0%	0.0%	0.0%	0.0%
d18:0	C ₁₈ H ₃₉ NO ₂	302.306	0.4%	0.3%	0.5%	0.6%	0.6%	1.1%	0.3%	0.1%	0.3%	0.3%
d18:1	C ₁₈ H ₃₇ NO ₂	300.290	13.7%	14.3%	14.1%	14.3%	11.6%	9.2%	13.9%	14.1%	13.7%	14.7%
d18:2	C ₁₈ H ₃₅ NO ₂	298.275	73.6%	73.2%	72.5%	69.4%	51.5%	35.8%	73.5%	72.7%	73.9%	74.3%
d18:3	C ₁₈ H ₃₃ NO ₂	296.259	0.2%	0.2%	0.2%	0.2%	0.4%	0.3%	0.2%	0.2%	0.1%	0.1%
d19:2	C ₁₉ H ₃₇ NO ₂	312.290	2.3%	2.4%	2.4%	2.3%	1.4%	1.0%	2.4%	2.4%	2.1%	2.0%
d19:3	C ₁₉ H ₃₅ NO ₂	310.275	4.9%	4.7%	4.7%	5.0%	5.0%	3.8%	4.8%	5.1%	4.6%	2.6%

Supporting Table S2: Primers used in this study

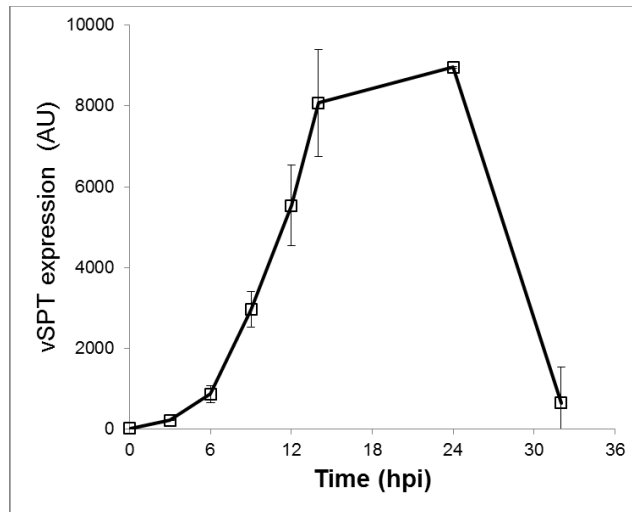
Gene name	Gene ID (NCBI)	Forward primer	Reverse primer	Reference
<i>mcp</i>	EPVG_00083	ACGCACCCTCAAT GTATGGAAGG	AGCCAACCTCAGCAGT CGTTC	(1)
<i>vSPT</i>	EPVG_00048	AGTCCGGTATCGT CTTGTCG	CGCAATGCGATAATA CATGG	(2)
<i>hSPT</i>	KJ868221.1	ACTGATTCCTCC GCATGAC	CGATGCCAAACGAGT AGATG	(2)
<i>β-tubulin</i>	GQ232273.1	CGCTGTACGACAT CTGCTT	GGAAGGGGATCATGT TGAC	(2)

Supporting Figures

B	B Ions	B+2H	B-NH3	B-H2O	AA	Y Ions	Y+2H	Y-NH3	Y-H2O	Y
1	130.0			112.0	E	1,826.9	913.9	1,809.9	1,808.9	15
2	258.1		241.1	240.1	Q	1,697.8	849.4	1,680.8	1,679.8	14
3	371.2		354.2	353.2	L	1,569.8	785.4	1,552.8	1,551.8	13
4	486.2		469.2	468.2	D	1,456.7	728.9	1,439.7	1,438.7	12
5	649.3		632.3	631.3	Y	1,341.7	671.3	1,324.6	1,323.7	11
6	748.4	374.7	731.3	730.3	V	1,178.6	589.8	1,161.6	1,160.6	10
7	861.4	431.2	844.4	843.4	L	1,079.5	540.3	1,062.5	1,061.5	9
8	1,008.5	504.7	991.4	990.5	M+16	966.5	483.7	949.4	948.4	8
9	1,107.5	554.3	1,090.5	1,089.5	V	819.4	410.2	802.4	801.4	7
10	1,220.6	610.8	1,203.6	1,202.6	I	720.4	360.7	703.3	702.3	6
11	1,335.7	668.3	1,318.6	1,317.6	D	607.3		590.2	589.3	5
12	1,464.7	732.9	1,447.7	1,446.7	E	492.2		475.2	474.2	4
13	1,565.7	783.4	1,548.7	1,547.7	T	363.2		346.2	345.2	3
14	1,652.8	826.9	1,635.7	1,634.8	S	262.2		245.1	244.1	2
15	1,826.9	913.9	1,809.9	1,808.9	R	175.1		158.1		1

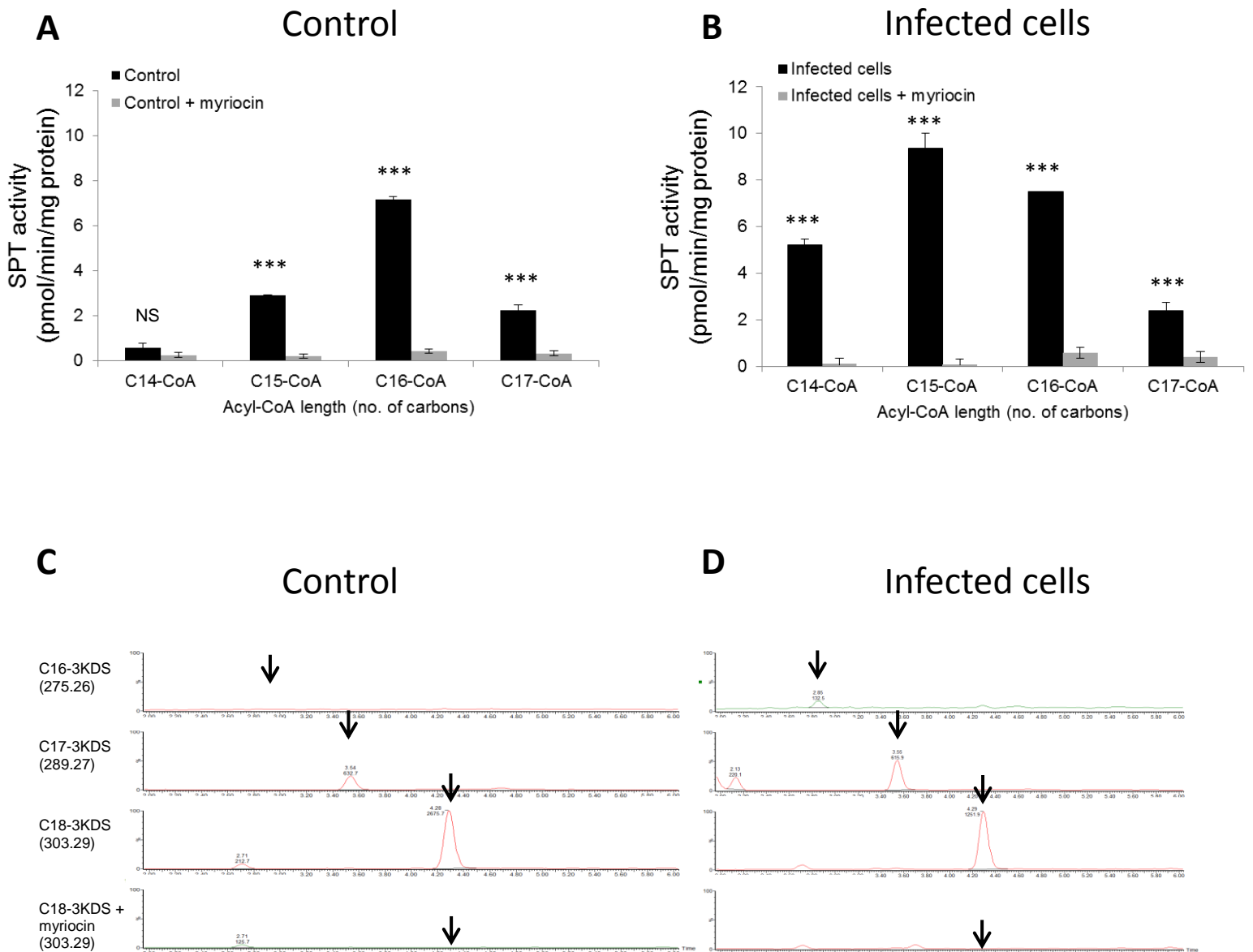


Supporting Figure S1: Mass-spec identification of vSPT protein resolved on SDS-PAGE. A signal peptide found in the vSPT protein was identified with over 95% probability (Expected value 0.0092). The collision induced dissociation MS/MS fragmentation table and spectrum of this peptide: (r)-EQLDYYYLoMVIDETSR (where o indicates oxidation of the met residue) are presented.



Supporting Figure S2: Viral SPT is highly expressed at early stages of viral infection.

Quantification of Western blot analysis of protein extracts from infected *E. huxleyi* cultures (microsomal fraction) during the course of viral infection as detected with the anti-vSPT antibody. Average +/- SD of two biological replicates.

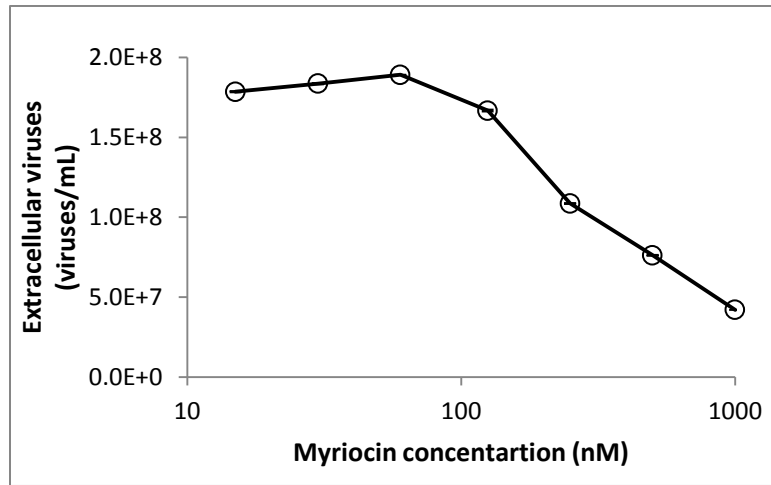


Supporting Figure S3: Viral infection induces a shift in substrate specificity of SPT *in vitro*. SPT enzymatic activity as determined by an *in vitro* assay performed with different acyl-CoAs and labeled Ser:

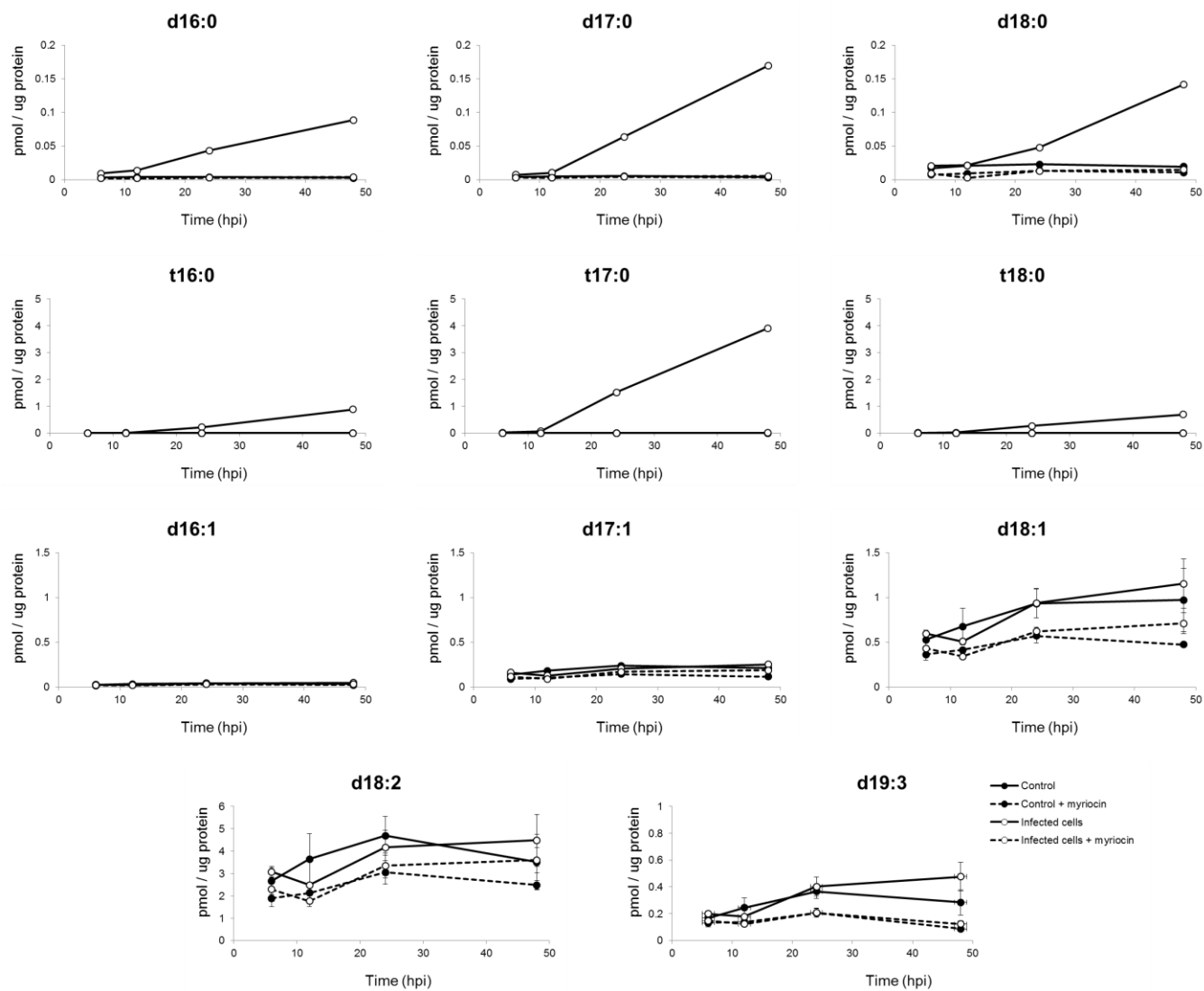
Top panel (A-B): Assay performed with four different acyl-CoAs (C14-CoA, C15-CoA, C16-CoA or C17-CoA) and radiolabeled Ser as substrates in the presence or absence of 1 μ M myriocin (a specific inhibitor of SPT). The samples assayed were the microsomal fraction of protein extracts from *E. huxleyi* control cultures (A) or infected cultures 14 hpi

(B). Statistical significance was determined by unpaired T test for each substrate against its myriocin treatment. Not significant (NS), * $P < 0.05$, ** $P < 0.01$ and *** $P < 0.001$.

Bottom panel (C-D): LC-MS chromatograms showing the peaks of the accurate mass (specified in parenthesis) of the labeled 3-KDS produced by SPT enzymatic activity performed *in vitro* with three acyl-CoAs (C14-CoA, C15-CoA and C16-CoA) and D₃-¹⁵N-Ser as substrates in the presence or absence of 1 μM myriocin. The samples assayed were the microsomal fraction of protein extracts from *E. huxleyi* control cultures (C) or infected cultures 12 hpi (D).

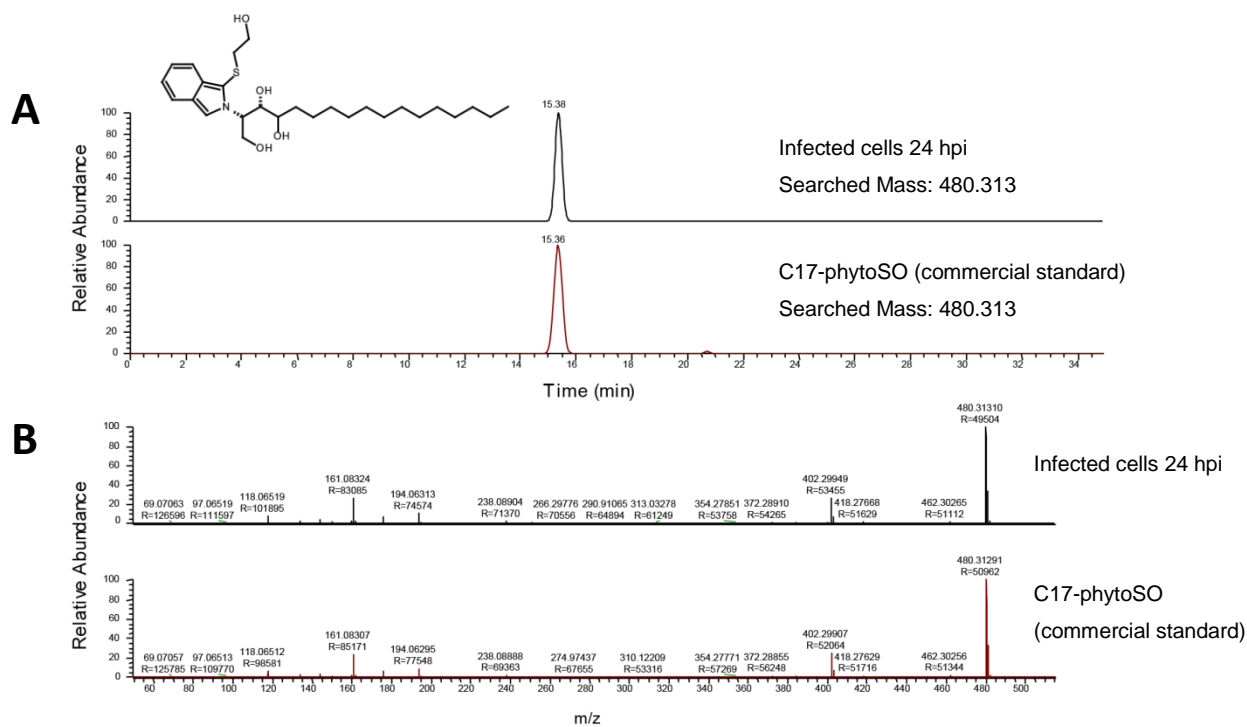


Supporting Figure S4: *de novo* LCB synthesis by the virus is required for viral assembly. Quantification of extracellular viral production of *E. huxleyi* infected culture, supplemented with different concentrations of myriocin, 20 hpi. Note the logarithmic scale of the x axis. The results presented are the average +/- SD of three biological replicates.



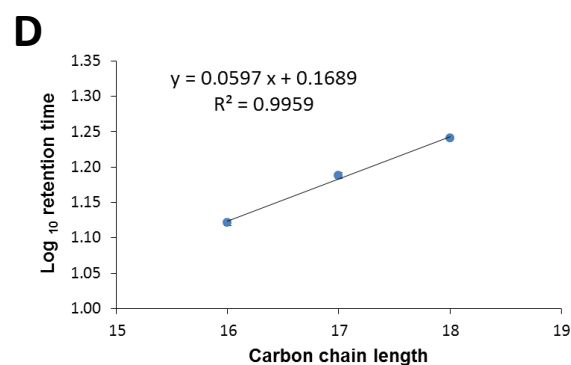
Supporting Figure S5: LCB profile during viral infection.

LC-MS quantification of different LCB species detected in *E. huxleyi* control and infected cultures during the course of infection. Cultures were supplemented with 1 μ M myriocin at the time of infection. The results presented are the average of three biological replicates \pm SD.



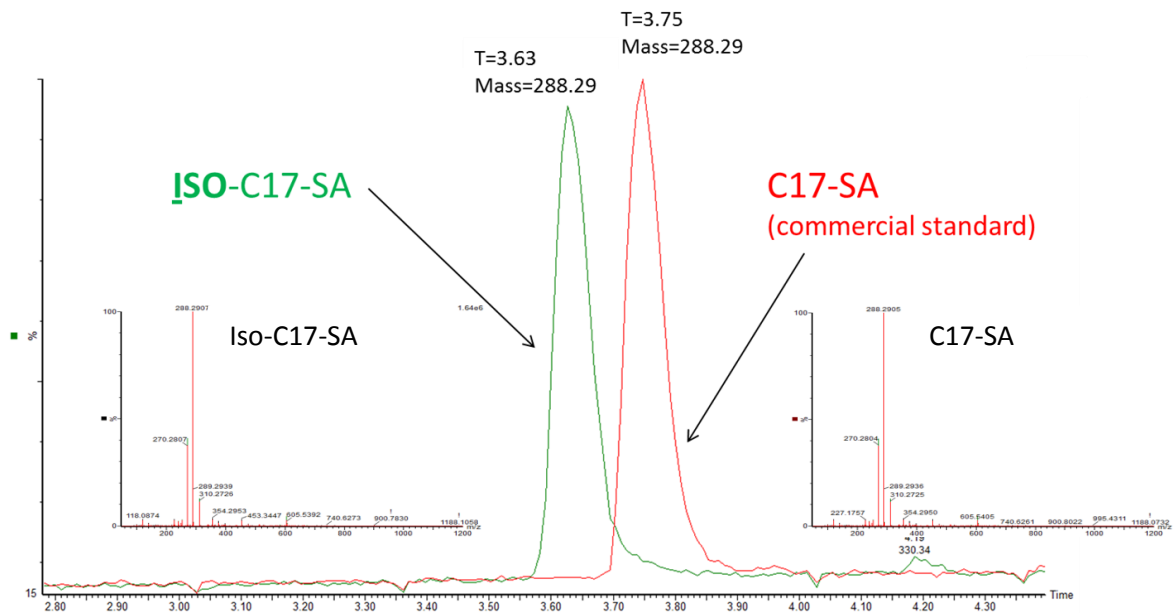
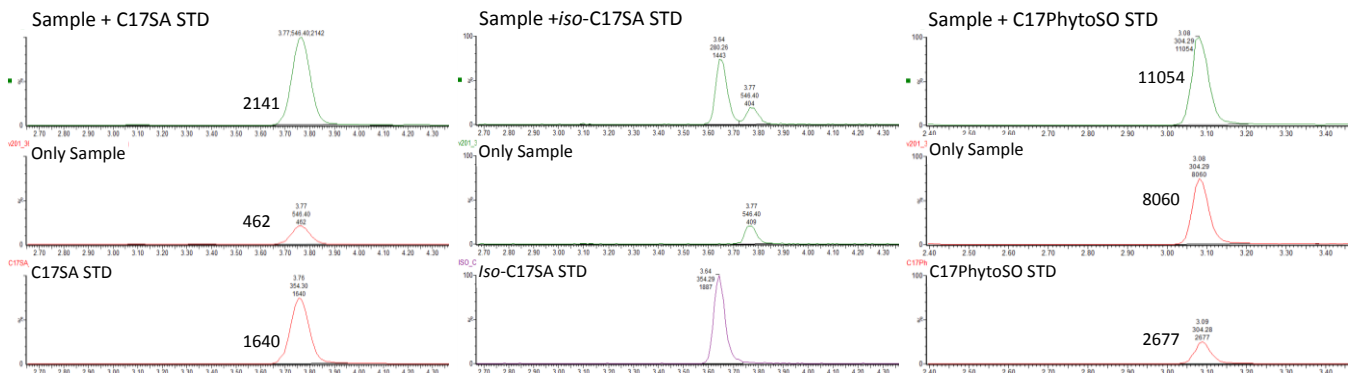
C

Sample (OPA-derivatized t17:0)		Synthetic standard (OPA-derivatized C17PhytoSO)		Molecular Ion	Molecular formula	Mass Error (ppm) sample t17:0 to synthetic C17PhytoSO std
m/z	Relative Intensity (%)	m/z	Relative Intensity (%)			
480.3131	100	480.3129	100	[M+H] ⁺	C ₂₇ H ₄₅ N ₁₀ O ₄ S ₁	0.4
462.3027	1.77	462.3026	1.55	[M+H] ⁺ (-H ₂ O)	C ₂₇ H ₄₃ N ₁₀ O ₃ S ₁	0.2
418.2767	1.65	418.2763	1.46			0.9
403.3035	7.12	403.3025	7.25			2.6
402.2995	26.26	402.2991	24.91	[M+H] ⁺ (-C ₂ H ₆ O ₅)	C ₂₅ H ₃₉ N ₁₀ O ₃	1.0
372.2891	1.27	372.2886	1.43			1.5
238.089	2.29	238.0889	2.2			0.7
194.0631	10.68	194.063	8.67			0.9
176.0703	6.83	176.0702	6.17			0.2
162.0866	2.78	162.0864	2.12			0.9
161.0832	26.05	161.0831	22.81			1.1
160.0754	2.57	160.0753	2.16			1.1
150.037	1.59	150.0368	1.1			1.0
144.0806	4.02	144.0804	3.49			1.0
134.0599	2.52	134.0598	2.39			0.4
118.0652	7.57	118.0651	6.68			0.6



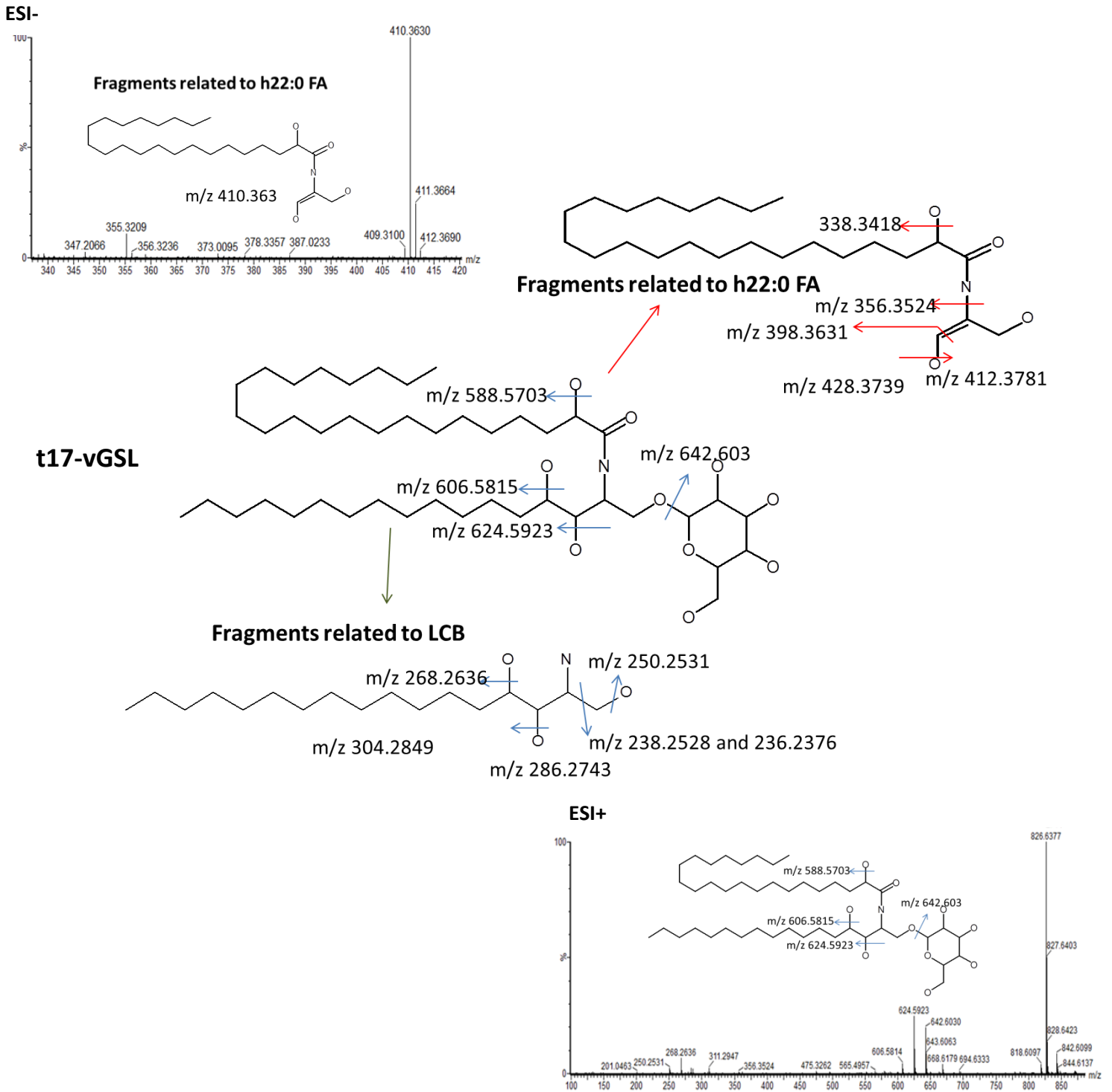
Supporting Figure S6: Putative structural elucidation of t17:0 after acid and base hydrolysis and derivatization with o-phathaldelyde.

LC-MS chromatograms (A) and fragmentation pattern (B) of t17:0 LCB detected in *E. huxleyi* infected cultures 24hpi (upper panel) as compared to commercial standard (Avanti polar lipids) of C17-phytoSO (lower panel) showing the same retention time and fragmentation. The list of fragments of both peaks is shown (C) demonstrating that all the fragments of the t17:0 sample are within ± 2 ppm as compared to synthetic control. The retention times of C16-, C17- and C18-phytoSO are plotted against carbon chain length (D) showing the expected linear relationship between carbon chain length and the logarithm of the retention time observed for phytoSO in samples as well as commercial standards.

A**B**

Supporting Figure S7: Viral infection induces the formation of C17 linear LCB and not C17 iso-branched.

(A) LC-MS overlay chromatograms and fragmentation pattern of *iso*-C17 sphinganine and C17-SA (commercial standard) show identical fragmentation but different retention time. (B) Lipid sample extracted from infected culture (36 hpi) was hydrolyzed (acid and base hydrolysis without derivatization) and was analyzed by LC-MS with or without LCB standard spiked into the sample. This Spiking experiment indicated that viral infection probably results in the synthesis of C17 linear sphinganine and C17 linear phytoSO (see methods). Numbers next to peaks indicate area integrated under the peak.

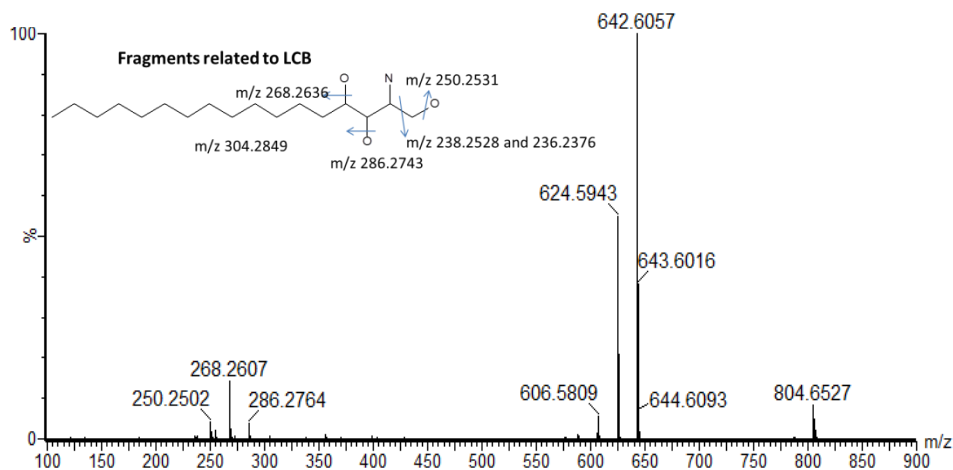


Supporting Figure S8: LC-MS putative identification of t17-vGSL (Glu-t17:0;h22:0).

Putative structure and expected fragmentation of t17-vGSL (Glu-t17:0;h22:0) as was analyzed by HPLC-MS both with ESI- (negative resolution mode) and ESI+ (positive resolution mode).

Positive mode:

ESI+ MS/MS of 804.65



ESI+	Empirical Formula	Theoretical mass	Detected MS/MS	Mass Error for MS/MS (ppm)	MS ^E	Mass Error for MS ^E (ppm)
[M+H] ⁺	C ₄₅ H ₉₀ NO ₁₀	804.6565	804.6544	-2.6	804.6544	-2.6
[M+Na] ⁺	C ₄₅ H ₈₉ NO ₁₀ Na	826.6384	826.637	-1.7	826.637	-1.7
[M+H-Glu] ⁺	C ₃₉ H ₈₀ NO ₅	642.6036	642.6057	3.3	642.603	-0.9
[M+H-Glu-H ₂ O] ⁺	C ₃₉ H ₇₈ NO ₄	624.5931	624.5943	1.9	624.5923	-1.3
[M+H-Glu-2H ₂ O] ⁺	C ₃₉ H ₇₆ NO ₃	606.5825	606.5809	-2.6	606.5815	-1.6
[M+H-Glu-3H ₂ O] ⁺	C ₃₉ H ₇₄ NO ₂	588.572	588.5665	-9.3	588.5703	-2.9
[LCB+H] ⁺	C ₁₇ H ₃₈ NO ₃	304.2852	304.2836	-5.3	304.2849	-1.0
[LCB+H-H ₂ O] ⁺	C ₁₇ H ₃₆ NO ₂	286.2746	286.2764	6.3	286.2743	-1.0
[LCB+H-2H ₂ O] ⁺	C ₁₇ H ₃₄ NO	268.264	268.2607	-12.3	268.2636	-1.5
[LCB+H-3H ₂ O] ⁺	C ₁₇ H ₃₂ N	250.2535	250.2502	-13.2	250.2531	-1.6
[LCB+H-3H ₂ O-CH ₂ +H ₂] ⁺	C ₁₆ H ₃₂ N	238.2535	238.2563	11.8	238.2528	-2.9
[LCB+H-3H ₂ O-CH ₂] ⁺	C ₁₆ H ₃₀ N	236.2378	236.2402	10.2	236.2376	-0.8
FA Derivative1	C ₂₅ H ₅₀ NO ₄	428.374	428.3726	-3.3	428.3739	-0.2
FA Derivative2	C ₂₅ H ₅₀ NO ₃	412.3791	412.378	-2.7	412.3781	-2.4
FA Derivative3	C ₂₄ H ₄₈ NO ₃	398.3634	398.3667	8.3	398.3631	-0.8
FA Derivative4	C ₂₂ H ₄₆ NO ₂	356.3529	356.3511	-5.1	356.3524	-1.4
FA Derivative5	C ₂₂ H ₄₄ NO	338.3423	338.3406	-5.0	338.3418	-1.5

Supporting Figure S9: LC-MS analysis of t17-vGSL (Glu-t17:0;h22:0).

A list of fragments detected with ESI+ (full scan MS^E positive resolution mode or MS/MS).

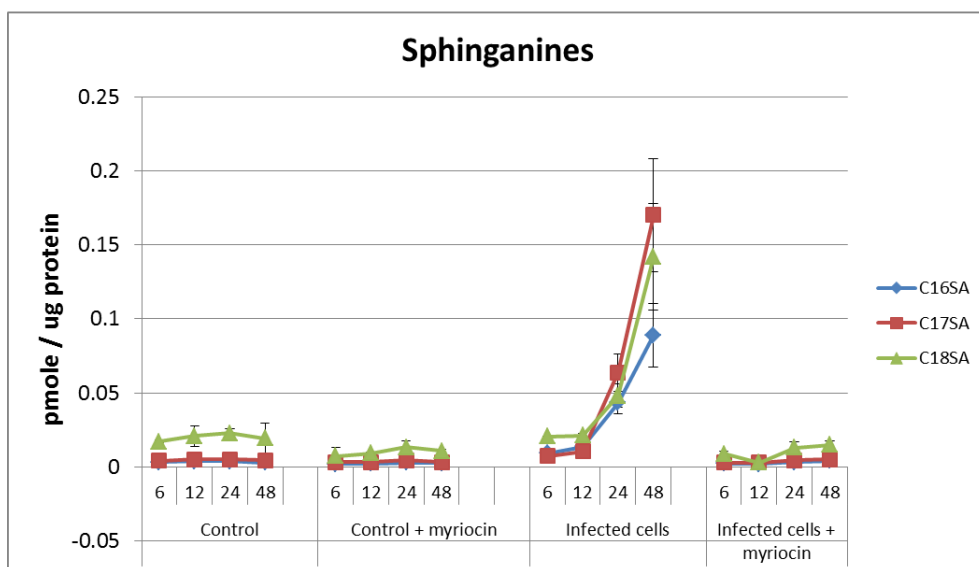
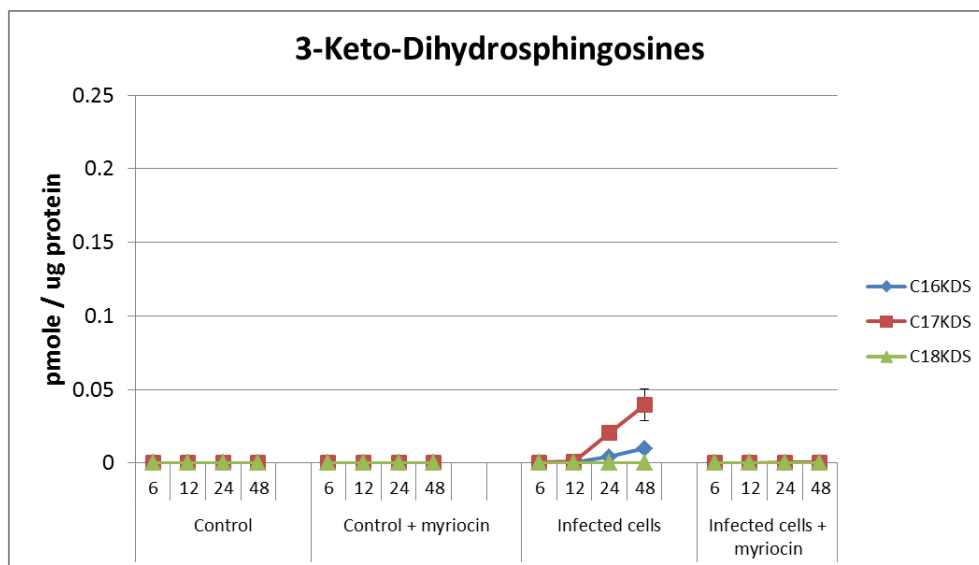
Negative mode:

ESI-	Empirical Formula	Theoretical mass	MS ^E	Mass Error (ppm)
[M-H]-	C45H88NO10	802.6408	802.6397	-1.4
[M+CH3COO]-	C47H92NO12	862.662	862.6605	-1.7
[M+HCOO]-	C46H90NO12	848.6463	848.6436	-3.2
[M-H-Glu]-	C39H78NO5	640.588	640.5861	-3.0
[M-H-Glu-H2O]-	C39H76NO4	622.5774	622.5767	-1.1
[M-H-Glu-2H2O]-	C39H74NO3	604.5669	604.5667	-0.3
FA Derivative2	C25H48NO3	410.3634	410.363	-1.0
FA Derivative3	C24H46NO3	396.3478	396.3473	-1.3
[FA h22:0]-	C22H43O3	355.3212	355.3209	-0.8
[FA h22:0-H2O]-	C22H41O2	337.3107	337.3093	-4.2

Supporting Figure S10: LC-MS analysis of t17-vGSL (Glu-t17:0;h22:0).

A list of fragments detected with ESI- (full scan MS^E negative resolution mode)

Note that in negative ion mode, LCB fragments cannot be detected.



Supporting Figure S11: 3-Keto-Dihydrospingosines (KDS) with 16 or 17 carbons in length were accumulated during viral infection

LC-MS analysis indicated the accumulation of C16 and C17 KDS but not C18 KDS during viral infection (top chart). Note that no KDS species were identified in non-infected control cells and the accumulation of the KDS species during viral infection was completely abolished upon myriocin inhibition of SPT. Sphinganines (bottom chart) were also found to be accumulated during viral infection in a myriocin dependent manner.

Supporting Methods

Enumeration of Cell and Virus Abundance

Cells were monitored and quantified using an Eclipse (iCyt) flow cytometer (Sony Biotechnology, Weybridge, UK), equipped with 405- and 488-nm solid state air-cooled lasers (both 25 mW on the flow cell) and standard filter setup. Algae were identified by plotting chlorophyll fluorescence in the red channel (737 to 663 nm) versus green fluorescence (500 to 550 nm) or side scatter. For extracellular viral production, samples were fixed with a final concentration of 0.5% glutaraldehyde for 30 min at 4°C, plunged into liquid nitrogen, and stored at -80°C until analysis. After thawing, 2:75 ratio of fixed sample was stained with SYBR gold (Invitrogen, Paisley, UK) prepared in Tris-EDTA buffer as instructed by the manufacturer (5 µL SYBR gold in 50 mL Tris-EDTA), then incubated for 20 min at 80°C and cooled down to room temperature. Flow cytometric analysis was performed with excitation at 488- and 525-nm emission. For intracellular viral DNA quantification, 1 mL cells was collected by centrifugation (8000 g, 3 min, 4°C) and washed twice in fresh media, and the DNA was released from cells using a REExtract-N-Amp Plant PCR kit (Sigma-Aldrich, Rehovot, Israel) according to the manufacturer's instructions. The extract was diluted 100× in double distilled water, and 1 µL was used for quantitative PCR analysis with the major capsid protein (*mcp*) primers (1). All reactions were performed in biological triplicates and technical duplicates. For all reactions, Platinum SYBR Green qPCR SuperMix-UDG with ROX (Invitrogen, Paisley, UK) was used as described by the manufacturer. Reactions were performed on StepOnePlus real-time PCR systems (Applied Biosystems, Foster City, CA) as follows: 50 °C for 2 min, 95°C for 2 min, 40 cycles of 95°C for 15 s, and 60°C for 30 s. Results were calibrated against serial dilutions of EhV201 DNA at known concentrations, enabling exact enumeration of viral abundance.

RNA Isolation and cDNA synthesis

RNA was isolated from 100 mL cultures at time points as indicated with the RNeasy Plant Mini kit (Qiagen, Foster City, CA) according to the manufacturer's instructions, followed by DNase treatment with Turbo DNase (Ambion, Carlsbad, CA). Equal amounts of RNA were used for cDNA synthesis with the Verso RT-PCR system (Thermo Fisher Scientific, Carlsbad, CA) following the manufacturer's instructions using a mixture of poly(T) oligo and random hexamers as primers. For transcript abundance analysis, Platinum SYBR Green qPCR SuperMix-UDG with ROX (Invitrogen, Paisley, UK) was used as described by the manufacturer. Primers used for the detection of the different transcripts are summarized in Supporting Table S2. Reactions were performed on StepOnePlus real-time PCR Systems as follows: 50°C for 2 min, 95°C for 2 min, 40 cycles of 95°C for 15 s, 60°C for 30 s. Transcript abundance was calculated by normalizing the results to expression of β -tubulin in each sample and to the expression of the control (uninfected) sample at the same time point.

Protein extraction and analysis

Preparation of microsomes

Fractionation of soluble and membrane fractions were carried out as in (3), with minor changes. Essentially, *E. huxleyi* whole-cell extracts were prepared from 300 mL cultures at 10^6 cells mL⁻¹ that were centrifuged (10,000 g for 15 min at 4°C) and plunged into liquid nitrogen. Cells were then re-suspended in lysis buffer (150 mM NaCl, 1 M Tris pH = 8, 0.5 M EDTA) and lysed by sonication (5 × 5.5 s cycles). Samples were centrifuged (500 g for 5 min at 4°C) to remove cell debris. The supernatant was centrifuged at 15,000 g for 15 min at 4°C to generate the membrane fraction. For SPT solubilization, the membrane pellet fraction was re-suspended in lysis buffer containing Sucrose monolaurate (SML, Sigma-Aldrich, Rehovot, Israel).

Immunoblot assays

A pellet of 300 mL of cells was re-suspended in lysis buffer supplemented with SML and sonicated to extract whole-cell proteins. Before loading of the proteins, cell debris was removed from the protein extracts by centrifugation (500 g for 5 min at 4°C). Proteins (40 µg protein per lane) were separated with 6 M urea sodium dodecyl sulfate polyacrylamide gel electrophoresis (SDS-PAGE) and blotted onto polyvinylidene difluoride (PVDF) membranes.

The primary anti-vSPT antibody was raised against the peptide ERDYDVYHELNN in rabbits and subsequently affinity-purified by the same synthetic peptide (Sigma-Aldrich, Rehovot, Israel). The anti-vSPT antibody and the secondary horseradish peroxidase-conjugated anti-rabbit antibody (Sigma-Aldrich, Rehovot, Israel) were diluted 1 : 2000 and 1 : 20000, respectively, in Tris-buffered saline containing 0.1% Tween 20 and 5% milk powder. The ECL-Prime western blotting detection reagent (GE Healthcare) was used for detection.

In-gel Digestion and Protein Identification by LC-ESI-MS/MS

In-gel Digestion

Protein bands were excised from the SDS gel stained with coomassie. The protein bands were subsequently reduced, alkylated and in-gel digested with trypsin (Promega, Madison, WI) at a concentration of 12.5 ng/µl in 50 mM ammonium bicarbonate at 37°C, as described by (4). The peptide mixtures were extracted with 80% CH₃CN, 1% CF₃COOH, and the organic solvent was evaporated in a vacuum centrifuge. The resulting peptide mixtures were reconstituted in 80% Formic Acid and immediately diluted 1:10 with Milli-Q water prior to the analysis by online reverse-phase nano-LC (liquid chromatography) - electro spray ionization (ESI) tandem mass spectrometric analyses (MS/MS).

Mass Spectrometry

LC–MS/MS was performed using a 15 cm fused-silica capillary column (inner diameter 75 μm) made in-house and packed with 3 μm ReproSil-Pur C18AQ media (Dr. Maisch GmbH). Samples were applied to an UltiMate 3000 Nano LC System, (Dionex). The LC system was used in conjunction with an LTQ Orbitrap XL mass spectrometer (Thermo Fisher Scientific) operated in the positive ion mode and equipped with a nanoelectrospray ion source. Peptides were separated with a 120 minute gradient from 3% to 35% acetonitrile (buffer A, 5% acetonitrile, 0.1% formic acid and 0.005% TFA; buffer B, 90% acetonitrile, 0.2% formic acid and 0.005% TFA). The voltage applied to the union to produce an electrospray was 1.2 kV. The mass spectrometer was operated in the data-dependent mode. Survey mass spectrometry scans were acquired in the Orbitrap with the resolution set to a value of 60,000. Up to the seven most intense ions per scan were fragmented and analyzed in the linear ion trap. Raw data files were searched with MASCOT (Matrix Science London, UK) against a modified Swissprot database containing the vSPT protein. Search parameters included a fixed modification of 57.02146 Da (carboxyamidomethylation) on Cys, and variable modifications of 15.99491 Da (oxidation) on Met and 0.984016 Da (deamidation) on Asn and Gln. The search parameters were as follows: Trypsin was used for the enzyme, maximum 2 missed cleavages, initial precursor ion mass tolerance 10 ppm, fragment ion mass tolerance 0.6 Da. Mascot results were further analyzed with Scaffold Proteome software (Portland, Oregon). The vSPT was validated by a peptide that was identified with over 95% probability (Supporting Fig. S1).

LCB analysis

To determine the LCB in cell cultures, cultures were sampled for 48 h, in addition to cultures where SPT enzymatic activity was inhibited by 1 μM myriocin. The inhibitor was added to the culture at time 0 (i.e. with the virus) and the cultures were sampled 6, 12, 24 and 48 hpi. The lipids were analysed as described before by (5) with some modifications. Briefly, 0.5 ml of methanol was added to 80 μg protein from the algae homogenate (PBS pH =7.4 with 0.2% v/v Triton X-100) and spiked with 200 pmol of the

internal standards d7-sphingosine and d7-sphinganine (d7SA, d7SO; Avanti Polar Lipids, Alabaster, AL). The mix was then incubated in a thermo-mixer at 37°C for one hour. Precipitated proteins were pelleted by centrifugation and the supernatant transferred to a new tube. For lipid hydrolysis, 75µl of methanolic HCl (1 N HCl and 10 M H₂O in methanol) was added to the supernatant and incubated for 16 hours at 65°C. This was followed by the addition of 100 µl of 10M KOH to neutralize the HCl and hydrolyze the phospholipids. To this mix, 625µl chloroform was added. Then, 100 µl 2N ammonium hydroxide and 0.5 ml alkaline water (500µl NH₄OH (2N) in 250ml H₂O) were added to complete the phase separation. The mix was then vortexed and centrifuged at 16000g for 5 minutes. After centrifugation, the upper phase was discarded and the lower organic phase was washed three times with alkaline water. Finally, the organic phase was dried under N₂ and kept at -20 °C until analysis. Before LC/MS analysis, the dried lipids were re-dissolved in 75 µl of methanol:ethanol:water mix (85:50:15 v/v) and derivatized with 5µl of 0.75mg o-phthalaldehyde in boric acid (pH = 10.3) and 7.5nl β-mercapto-ethanol. The OPA-derivatized sphingoid bases were separated on a C₁₈ column (Uptisphere 120 Å, 5µm, 125 × 2 mm, Interchim, Montluçon, France) using a UPLC pump Transcend (Thermo, Reinach, BL, Switzerland) with solvent A as methanol 50% in water with 5mM ammonium acetate and solvent B as 100% methanol. The following gradient was applied from 0- 25 minutes 100% solvent A to 50% solvent A, 25-31 min 100% solvent B and then 31-35 min 50% solvent A. The sphingoid bases were then detected on a hybrid quadrupole Orbitrap mass spectrometer Q-Exactive (Thermo, Reinach, BL, Switzerland) with atmospheric pressure chemical ionization (APCI) as the ionization source. Two scan modes were applied. Full scan mode with mass resolution of 140000, AGC target 3.00E+06, max injection time of 512 ms and scan range m/z 120-1200. For identification, targeted selected ion monitoring mode (parallel reaction monitoring) was applied with a target list containing 480.3 m/z (the m/z of OPA derivatized C17-phytoSO) and a control 494.3 (the m/z of the OPA derivatized C18-phytoSO) with settings: mass resolution of 140000, AGC target 2.00E+05, max injection time of 100 ms, scan range m/z 120-1200, in source CID of 10 eV and normalized stepped collision energy 10,20 and 30 eV. Mass calibration was checked using the internal standards for each run and was < 5 ppm.

This type of analysis enables the detection of free LCB as well as LCB that are incorporated into more complex sphingolipids. LCB species were detected according to their accurate mass and retention time (Supporting Table S1) in comparison to known standards. Quantification was done by normalizing the area under the peak of each sphingoid based to the internal standard (d7SO) in the full scan mode and to protein content of the sample, as determined by BCA assay for the cell lysate before the lipid extraction.

Sphingolipid Analysis

Lipids were extracted from *E. huxleyi* cells infected with EhV201 and from non-infected cells harvested at 12, 24, 32, and 48 hpi in three biological replicates of 50 mL. Lipid analysis was performed as previously described in (6) with some modifications: filters containing algae were placed in 15 mL glass tubes and extracted with 3 mL of a pre-cooled (-20°C) homogenous methanol:methyl-tert-butyl-ether (TMBE) 1:3 (v/v) mixture containing $0.1\mu\text{g/mL}$ of glucosylceramide (d18:1/12:0) which was used as an internal standard. The tubes were shaken for 30 minutes at 4°C and then sonicated for 30 minutes. UPLC grade water: methanol (3:1, v/v) solution (1.5 mL) was added to the tubes followed by centrifugation. The upper organic phase (1.2 mL) was transferred in to 2 mL Eppendorf tube. The polar phase containing algae debris and filter pieces was re-extracted with 0.5 mL of TMBE. Organic phases were combined and dried under N_2 stream and then stored at -80°C until analysis. The dried lipid extracts were re-suspended in 300 μL buffer B (see below) and centrifuged again at 13,000 rpm and 4°C for 5 min.

For the spiking experiment, lipids were extracted as described from 600 ml cultures control as well as of viral infected algae (36 hpi) in duplicates, then hydrolyzed by acid/base hydrolysis (7). The resulting LCB were analyzed by LC-MS without further derivatization. Equal amounts of sample were analyzed alone or with known amount of commercial standard that was added to the sample prior to being injected to the LC/MS.

UPLC-q-TOF MS for sphingolipid analysis

Post extraction, the supernatant was transferred to an autosampler vial and an aliquot was subjected to UPLC-MS (Ultra performance liquid chromatography - mass spectrometry) analysis. Lipid extracts were analyzed using a Waters ACQUITY UPLC system coupled to a SYNAPT G2 HDMS mass spectrometer (Waters Corp., Milford, MA). Chromatographic conditions were as described in Hummel *et al.* 2011 (6). Briefly, the chromatographic separation was performed on an ACQUITY UPLC BEH C8 column (2.1×100 mm, i.d., 1.7 μm) (Waters Corp., Milford, MA). The mobile phase consisted of water (UPLC grade) with 1% 1 M NH₄Ac, 0.1% acetic acid (mobile phase A), and acetonitrile:isopropanol (7:3) with 1% 1 M NH₄Ac, 0.1% acetic acid (mobile phase B). The column was maintained at 40°C and flow rate of mobile phase was 0.4 mL/min. MS parameters were as follows: the source and de-solvation temperatures were maintained at 120°C and 450°C, respectively. The capillary voltage and cone voltage were set to 1.0 kV and 40 V, respectively. Nitrogen was used as de-solvation gas and cone gas at the flow rate of 800 L/h and 20 L/h, respectively. The mass spectrometer was operated in full scan MS^E positive resolution mode over a mass range of 50 Da-1500 Da. For the high energy scan function, a collision energy ramp of 15-35 eV was applied, for the low energy scan function -4 eV was applied. Leucine-enkephalin was used as lock-mass reference standard. The major ions and specific fragment ions of the lipid were analyzed in positive ionization mode. For identification of vGSL, extracts of infected cells were injected by using both positive and negative ionization modes. The MS^E energies applied for the negative ionization were 10-30 eV. For MS/MS (in positive ionization mode), collision energy ramp of 10-40 eV was applied.

Data Analysis, lipid identification and quantification

LC-MS data were analyzed and processed by using QuanLynx (Version 4.1, Waters Corp., Milford, MA). The putative identification of the different lipid species was performed according to the lipid accurate mass and fragmentation pattern. Further annotation of the lipids was based on the correlation between retention time (RT) and carbon chain length and degree of unsaturation. The validation of the putative

identification of sphingolipids was performed by comparing to home-made library which contains lipids produced by plants (*Arabidopsis*, tomato etc.) and algae. The metabolites were integrated using the QuanLynx tool incorporated in MassLynx. Areas of metabolites were normalized to the area of the IS and to the amount of algae used for analysis.

The identity of the most abundant t17-vGSL, MonohexosylCer (t17:0/h22:0), was verified according to the expected masses (Supporting Fig. S8-S10) and with full scan MS^E over two magnitudes of collision energy. The fragmentation pattern was analyzed by ESI in negative (Supporting Fig. S10) and positive mode (Supporting Fig. S9) and verified by MS/MS of molecular ion 804.6565 (M+H) in positive ionization mode.

Identification of hGSL (8) and sGSL (9) was performed according to the mentioned references. The GSLs and ceramides were detected as [M+H]⁺ and [M+Na]⁺. Neutral loss of head group and further loss of water were the specific fragment ions of GSLs. In addition, the long chain base (LCB) and fatty acid related ions were also clearly observed as a characteristic signature of the ceramide backbone. The dehydration of ceramide was preferentially formed by the formation of a conjugated system on the ceramide backbone. The dominant fragment was the neutral loss of water molecular. Moreover, a second dehydration step and LCB related ions were also detected.

References

1. Pagarete A, Allen MJ, Wilson WH, Kimmance SA, & de Vargas C (2009) Host-virus shift of the sphingolipid pathway along an *Emiliana huxleyi* bloom: survival of the fattest. *Environ. Microbiol.* 11(11):2840-2848.
2. Rosenwasser S, et al. (2014) Rewiring host lipid metabolism by large viruses determines the fate of *Emiliana huxleyi*, a bloom-forming alga in the ocean. *Plant cell* 26(6):2689-2707.
3. Perez-Perez ME, Florencio FJ, & Crespo JL (2010) Inhibition of target of rapamycin signaling and stress activate autophagy in *Chlamydomonas reinhardtii*. *Plant Physiol.* 152(4):1874-1888.
4. Shevchenko A, Wilm M, Vorm O, & Mann M (1996) Mass spectrometric sequencing of proteins silver-stained polyacrylamide gels. *Anal Chem* 68(5):850-858.
5. Penno A, et al. (2010) Hereditary sensory neuropathy type 1 is caused by the accumulation of two neurotoxic sphingolipids. *J Biol Chem* 285(15):11178-11187.
6. Hummel J, et al. (2011) Ultra performance liquid chromatography and high resolution mass spectrometry for the analysis of plant lipids. *Front Plant Sci* 2:54.
7. Rutti MF, Richard S, Penno A, von Eckardstein A, & Hornemann T (2009) An improved method to determine serine palmitoyltransferase activity. *J Lipid Res* 50(6):1237-1244.
8. Vardi A, et al. (2012) Host-virus dynamics and subcellular controls of cell fate in a natural coccolithophore population. *Proc Natl Acad Sci USA* 109(47):19327-19332.
9. Fulton JM, et al. (2014) Novel molecular determinants of viral susceptibility and resistance in the lipidome of *Emiliana huxleyi*. *Environ Microbiol* 16(4):1137-1149.